THE JOURNAL OF PHYSICAL CHEMISTRY A LETTERS

2008, *112,* 10439–10441
Published on Web 09/30/2008

Ultrasensitive Absorption Spectroscopy of Optically-Trapped Aerosol Droplets

Kerry J. Knox and Jonathan P. Reid*

School of Chemistry, University of Bristol, Bristol BS8 1TS, U.K.

Received: August 19, 2008; Revised Manuscript Received: September 15, 2008

High-sensitivity optical absorption measurements on individual sub-picoliter aqueous droplets are reported using aerosol optical tweezers to simultaneously manipulate and characterize a sample droplet and a control droplet for comparison. It is demonstrated that the detection sensitivity to trace analytes is set by the weak absorption by the solvent, water, and that absorbances less than 5×10^{-7} can be measured over pathlengths of less than 10 μm. The potential applications of this approach to analyze aerosol particle composition and to perform trace analysis are discussed.

Optical absorption spectroscopy is a widely applied spectroscopic tool for chemical analysis and trace detection.[1,2] Measurements of light absorbance can allow the direct quantification of trace species without the need for external calibration, with the limit of detection (LOD) dependent on the sample path length and the molar extinction of the analyte. Recently, the development of micrototal analysis systems has increased the need for new techniques for trace analysis in small sample volumes over limited pathlengths.[3−5] Further, there is considerable environmental interest in developing new techniques for characterizing the chemical composition of natural and anthropogenic aerosols and for examining the optical properties of absorbing atmospheric particles.[6]

We present here a novel comparative approach for performing absorption spectroscopy on sub-picoliter samples, examining light absorption by aqueous droplets. We have recently demonstrated that optical tweezers can be used to manipulate and investigate the properties of two aerosol droplets in situ, allowing the hygroscopicity of the particles to be compared with variation in gas phase relative humidity (RH).[7,8] Although the droplets are trapped by light, the imaginary part of the refractive index of the aerosol water−solute solutions (k) is near a minimum at the visible wavelength used to trap the droplet, minimizing the perturbation of droplet temperature through optical absorption.[9,10] In this publication, we demonstrate that measurements of equilibrium droplet size with variation in optical irradiance can allow an estimation of the perturbation in droplet temperature and, hence, absorbance. Absorbances of $<5 \times 10^{-7}$ are measured over an optical path length of <10 μm.

The application of optical tweezers in measurements of aerosol properties has been discussed previously.[11,12] Briefly, a continuous-wave laser (532 nm) is focused by a 100× oil immersion objective through a coverslip into a custom-fabricated cell. Aerosol is introduced into the cell using a medical nebulizer, and droplets passing near the beam focus are captured by the strong optical gradient force. The laser power at the trap site is estimated using a second objective to recollimate the light after the trap for measurement with a power meter.[13] Two droplets can be independently manipulated by dividing the laser beam using a beam-splitter to form two traps separated by <100 μm. Droplets of identical composition can be captured in both traps, or droplets of different composition can be loaded sequentially. Backscattered Raman light from both droplets is collimated by the objective and imaged into a spectrograph. The dispersed Raman light is spatially resolved on the charge-coupled device (CCD) detector, recording spectroscopic fingerprints from both droplets concurrently with 1 s time resolution.

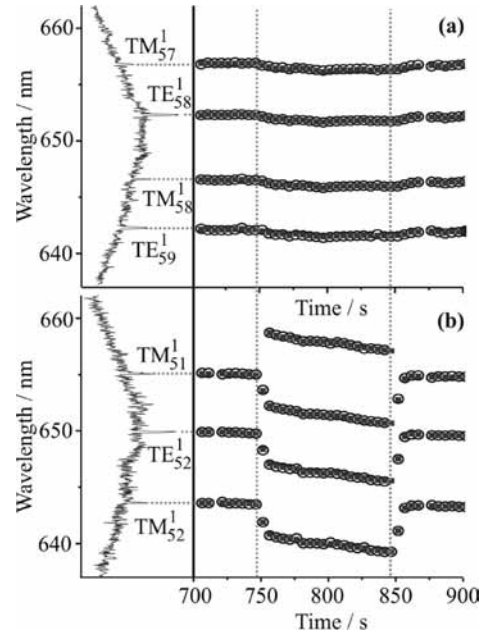

Figure 1. (a) The evolving WGM wavelengths of the control droplet between 700 and 900 s (right panel; small closed squares: calculated wavelengths; large open circles: recorded wavelengths) and the Raman fingerprint at 700 s (left panel). (b) The same as part a, but for the sample droplet.

The evolving Raman fingerprints of two aqueous sodium chloride droplets are compared in Figure 1, and the spectrum of each is shown at 700 s after capture. Each spectrum arises from excitation of the OH stretching vibrations of water (Stoke's

* Corresponding author.

10.1021/jp807418g CCC: $40.75

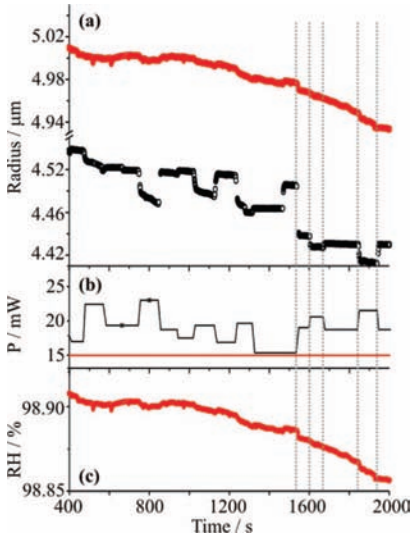

Figure 2. (a) The evolving sizes of the control (closed circles, top) and sample (open circles, lower) droplets. (b) The time dependence of the trap powers for each droplet (variable line: sample droplet; constant line: control droplet). (c) The ambient RH, as determined from the control droplet size and solute mass.

shift ~ 3500 cm^{-1}) and consists of a broad spontaneous Raman band and superimposed resonant structure at wavelengths commensurate with whispering gallery modes (WGMs). The WGM wavelengths form a unique fingerprint that can be used to determine the droplet radius with nanometer accuracy.[11] The assignments of the resonant modes are indicated, with the superscript denoting the mode order, the subscript denoting the mode number, and the polarization denoted by TE (transverse electric) or TM (transverse magnetic). At a time of ~750 s, the laser power P of the beam holding one droplet (the "sample" droplet) is raised from 19.4 ± 1.0 to 23.1 ± 1.0 mW. The WGMs respond by shifting to shorter wavelength, consistent with a decrease in droplet size by ~20 nm and a loss of ~1.7 × 10^{11} water molecules from the droplet. The finite time required for the size change results from the time required to effect the power change by adjusting a neutral density filter used to control the power. Decreasing the power back to the initial value at ~850 s leads to an almost complete recovery in size (~2 nm lower). The beam trapping the second droplet (the "control" droplet) is held at a constant power of 15 mW throughout and the size shows a decrease by ~2 nm, confirming that the RH decreases marginally over time.

The complete record of measurements is shown in Figure 2. The trapping power is varied by less than 50%, allowing absorption measurements to be made without significant perturbation in droplet temperature. Both droplets remain in equilibrium with the surrounding vapor at all times, but a declining RH is apparent from the long-time trend in the size of both droplets: the control droplet shows a steady decline in size by 74 nm over 1600 s. When the two droplets are first captured, it has been shown that they have a composition equal to that of the nebulized solution.[7] Consequently, the control droplet contains an estimated mass of solute of 10.5 pg, thereby allowing the variation in size with RH to be predicted from thermodynamic models.[7,9] Thus, the measured size at any time can be converted into an estimate of the RH with an accuracy of ± 0.09% and a high degree of precision: a 1 nm change in size corresponds to a change in RH of 6.8 × 10^{-4} %, a change in the water partial pressure of 0.014 Pa. The RH estimated from the control droplet size is shown in Figure 2c.

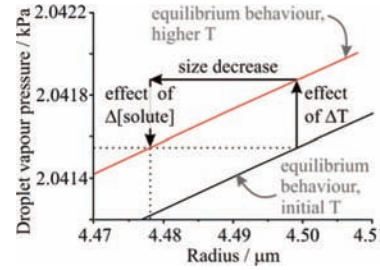

Figure 3. Schematic to illustrate the analytical approach used to determine the droplet temperature change associated with a given droplet size change.

Although the vertical position of the particle relative to the beam focus depends weakly on the trapping power,[11,12] the waist at the focus is considerably smaller than the droplet radius, R_d, and the entire irradiance passes through the droplet at all powers. Thus, the Beer−Lambert law can be applied to estimate the rate of heat generation by absorption (Q_{heat}, in J s^{-1}) over a path length equal to one droplet diameter, $2R_d$. At 532 nm k is 1.9 × 10^{-9}, corresponding to an absorption coefficient, α, of 4.3 × 10^{-4} cm^{-1}.[9,10] Assuming that water is the sole absorber in the droplet, the absorbance ($2R_d \times \alpha$) can be calculated to be 3.9 × 10^{-7}, and Q_{heat} is estimated from

$$Q_{heat} = (1 - \exp(-2R_d \cdot \alpha)) \times P \quad (1)$$

Absorption of this small fraction of incident energy leads to a perturbation in temperature, elevating the droplet above the ambient temperature. Thus, when the trap power is increased, the droplet temperature and vapor pressure both increase.

A Köhler curve, describing the change in the equilibrium vapor pressure of the droplet with radius, can be calculated for the sample droplet based on an estimate of the solute mass (Figure 3). An increase in temperature arising from an increase in power leads to an increased vapor pressure or partial pressure of water at the droplet surface. A concentration gradient is established, and water diffuses away from the droplet. Given the large volume of the surrounding bath gas, it is assumed that the surrounding RH is unaffected by such a small perturbation. Evaporation leads to a decrease in droplet size and an increase in solute concentration, lowering the vapor pressure and counteracting the increase from heating. Once the size has decreased sufficiently, the vapor pressure once again equals the surrounding RH and a new equilibrium size is established at a temperature that is elevated above the ambient. A larger elevation in temperature requires a larger reduction in size; conversely, a reduction in trap power leads to a decrease in the droplet temperature and an increase in size. Thus, a change in size can be related to a change in temperature. The vapor pressure of a dilute salt solution is assumed to show the same temperature dependence as pure water (144.95 Pa/K around 20 °C).[14] Given that an accuracy of 1 nm in the size measurement corresponds to an accuracy in the vapor pressure determination of 0.014 Pa, temperature changes as low as 0.1 mK could be observable using this approach. This would correspond to an evaporation or condensation of ~1 × 10^{10} molecules or a change of <0.1% in the droplet volume.

Although this discussion provides a qualitative description for the trend in equilibrium size with trapping power, it should be noted that this is not sufficient to interpret the data in Figure 2: it is essential to isolate the size changes arising from temperature perturbations from the more general trend arising from the change in RH. For this, an accurate measurement of the change in surrounding RH is supplied by the control droplet.

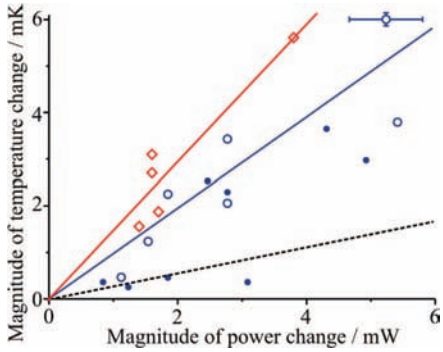

Figure 4. Magnitude of the measured droplet temperature change following change in trap power. Data in Figure 2 (solute concentration ~0.36 M): open circles show temperature changes following increases in power, along with a line of best fit (representative error bars shown for one point); closed circles show measurements following a decrease in power. Droplet of solute concentration 0.63 M: open diamonds and line. The dashed line shows the predicted temperature response for a pure water droplet.

From the temporal variation in the RH, we can have confidence in attributing the step changes in size of the sample droplet entirely to changes in absorption. The experimental data showing the perturbation in temperature with trap power change are presented in Figure 4. We see no evidence for enhanced absorption when the droplet size is resonant with the trapping wavelength.[15]

The rate of heat flow away from the droplet, Q_{cond}, (J s^{-1}) can be calculated from the steady heat flux away from the droplet at the surface, q (J s^{-1} m^{-2}), and the surface area of the droplet:

$$Q_{cond} = -q \times 4\pi {R_d}^2 = -K_a \left(\frac{\partial T}{\partial R}\right)_{R=R_d} \times 4\pi {R_d}^2 \qquad (2)$$

where K_a is the thermal conductivity of air (25.8×10^{-3} W m^{-1} K^{-1} at 295 K and 100 kPa).[14] When the droplet reaches an equilibrium size at the elevated temperature, the sum of the rate of heat generation and conduction away from the droplet must equal zero. Thus, the steady state temperature elevation above the ambient induced by a laser power P can be expressed as

$$\Delta T = \frac{(1 - \exp(-2R_d \cdot \alpha)) \times P}{4\pi R_d \cdot K_a} \qquad (3)$$

and the change in temperature accompanying a change in power can be predicted. Estimates for a water droplet ($\alpha \sim 4.3 \times 10^{-4}$ cm^{-1}) are compared with the experimental data in Figure 4.

These measurements demonstrate that it is possible to measure absorbances approaching $\sim 4 \times 10^{-7}$ over a path length of <10 μm. The data are consistent with a higher α than pure water (4.3×10^{-4} cm^{-1}): values of $(1.03 \pm 0.17) \times 10^{-3}$ and $(1.51 \pm 0.16) \times 10^{-3}$ cm^{-1} can be estimated from the data for power decreases and increases, respectively. The data recorded when the power is reduced have a fractionally larger error than those recorded when the power is increased; this will be investigated further in future work. The larger than expected value of α can be attributed to the presence of a trace concentration of absorbing impurities in the sodium chloride, at a salt concentration of 0.36 M in this measurement (Fisher Scientific, >99.5% purity). Data recorded in a second experiment at lower RH with a more concentrated solution droplet (0.63 M) are shown in Figure 4. The best estimate of α for this solution is $(2.39 \pm 0.19) \times 10^{-3}$ cm^{-1}, confirming that the absorbance of the solution increases with salt concentration. These data are consistent with an impurity concentration at the micromolar level with a molar absorption coefficient of 1000 M^{-1} cm^{-1}. If the absorption due to the solvent and impurities were to be reduced through use of a different solvent or change in wavelength, an absorbance 1 order of magnitude smaller should provide a resolvable size change. Recording such low absorbances would depend on the comparative nature of the measurement, through examining sample and control droplet size changes. This LOD compares well with recently reported values over pathlengths more than 1 order of magnitude larger. Zare and co-workers reported an LOD of $\sim 2 \times 10^{-7}$ over a path length of 300 μm using cavity ring-down spectroscopy and $\sim 3.5 \times 10^{-8}$ over 200 μm using coaxial thermal lensing.[16] Typical UV−vis absorption spectrometers exhibit a lower limit on the absorbance of 10^{-5} over millimeter pathlengths.

For direct measurements on aerosol samples, this technique represents a potentially valuable approach for examining the concentration of trace species within aerosols and probing the optical properties of weakly absorbing particles. Arnold et al. and Lin and Campillo reported absorption measurements on strongly absorbing single aqueous ammonium sulfate droplets ($\alpha \sim 10000$ cm^{-1}) excited at a wavelength of ~ 9 μm.[17,18] This work represents the first evidence that absorption spectroscopy is sensitive enough to probe trace constituents with low absorbances in micron sized, sub-picoliter aerosol droplets ($\alpha \sim 5 \times 10^{-4}$ cm^{-1}, a single scattering co-albedo of 2.5×10^{-7}). To broaden the applicability of the technique, this approach must be combined with new developments in aerosol sampling and manipulation, for example, the application of holographic optical tweezers to control aerosol arrays.[19,20]

Acknowledgment. The EPSRC is acknowledged for funding and for studentship support for K.J.K.

References and Notes

(1) Yoshihara, T.; Murai, M.; Tamaki, Y.; Furube, A.; Katoh, R. *Chem. Phys. Lett.* **2004**, *394*, 161.
(2) Hodgkinson, J.; Johnson, M.; Dakin, J. P. *Appl. Opt.* **1998**, *37*, 7320.
(3) Li, F. P.; Kachanov, A. A.; Zare, R. N. *Anal. Chem.* **2007**, *79*, 5264.
(4) Schwarz, M. A.; Hauser, P. C. *Lab Chip* **2001**, *1*, 1.
(5) Steigert, J.; Grumann, M.; Brenner, T.; Riegger, L.; Harter, J.; Zengerle, R.; Ducree, J. *Lab Chip* **2006**, *6*, 1040.
(6) Haywood, J.; Boucher, O. *Rev. Geophys.* **2000**, *38*, 513.
(7) Butler, J. R.; Mitchem, L.; Hanford, K. L.; Treul, L.; Reid, J. P. *Faraday Discuss.* **2008**, *137*, 351.
(8) Mitchem, L.; Hopkins, R. J.; Buajarern, J.; Ward, A. D.; Reid, J. P. *Chem. Phys. Lett.* **2006**, *432*, 362.
(9) Seinfeld, J. H.; Pandis, S. N. *Atmospheric Chemistry and Physics: From Air Pollution to Climate Change*; John Wiley and Sons: New York, 1998.
(10) Segelstein, D. The complex refractive index of water. M.S. Thesis, University of Missouri, Kansas City, MO, 1981.
(11) Mitchem, L.; Reid, J. P. *Chem. Soc. Rev.* **2008**, *37*, 756.
(12) Knox, K. J.; Reid, J. P.; Hanford, K. L.; Hudson, A. J.; Mitchem, L. *J. Opt. A* **2007**, *9*, 180.
(13) Viana, N. B.; Rocha, M. S.; Mesquita, O. N.; Mazolli, A.; Neto, P. A. M.; Nussenzveig, H. M. *Phys. Rev. E* **2007**, *75*, 021914.
(14) *The CRC Handbook of Chemistry and Physics*, 87th ed.; Lide, D. R., Ed.; CRC Press, Inc.: Boca Raton, FL, 2006.
(15) Popp, J.; Lankers, M.; Schaschek, K.; Kiefer, W.; Hodges, J. T. *Appl. Opt.* **1995**, *34*, 2380.
(16) Kuswandi, B.; Nuriman; Huskens, J.; Verboom, W. *Anal. Chim. Acta* **2007**, *601*, 141.
(17) Arnold, S.; Neuman, M.; Pluchino, A. B. *Opt. Lett.* **1984**, *9*, 4.
(18) Lin, H. B.; Campillo, A. J. *Appl. Opt.* **1985**, *24*, 422.
(19) Burnham, D. R.; McGloin, D. *Opt. Express* **2006**, *14*, 4175.
(20) Butler, J. R.; Wills, J. B.; Mitchem, L.; Burnham, D. R.; McGloin, D.; Reid, J. P. *Lab Chip*, submitted for publication, **2008**.

JP807418G